34th Annual International Conference of the IEEE EMBS
San Diego, California USA, 28 August - 1 September, 2012

Active Contour Based Segmentation for Insulin Granule Cores in Electron Micrographs of Beta Islet Cells

David Nam[1], Judith Mantell[2,3], Dave Bull[1], Paul Verkade[2,3,4*] and, Alin Achim[1*]

Abstract— **Transmission electron microscopy images of beta islet cells contain many complex structures, making it difficult to accurately segment insulin granule cores. Quantification of sub cellular structures will allow biologists to better understand cellular mechanics. Two novel, level set active contour models are presented in this paper. The first utilizes a shape regularizer to reduce oversegmentation. The second contribution is a dual active contour, which achieves accurate core segmentations. The segmentation algorithm proceeds through three stages: an initial rough segmentation using the first contribution, cleaning using morphological techniques and a refining step using the proposed dual active contour. Our method is validated on a set of manually defined ground truths.**

I. INTRODUCTION

As microscopes become more sophisticated and are able to achieve better resolutions, researchers are able to observe cellular processes in more detail. With the increased viewing power, new image processing algorithms need to be developed in order to extract as much information from the images as possible. Currently, scientists resort to slow, manual analysis to extract and analyze information from images. Image informatics has become the rate-limiting factor in realizing the full potential of dynamic cellular and molecular imaging studies [1]. Insulin is the only hormone in mammals able to lower blood glucose levels and subsequently it is vital for life. Disbalance of insulin levels may result in diabetes. Typically insulin granules are described as organelles containing a dense core, surrounded by a halo and an enclosing membrane, but this is very much dependent on the fixation procedure.

In this work, transmission electron microscopy (TEM) images of rat beta islet cells have been acquired to examine the physical dimensions of their insulin granule cores. Normally biologists use open source software, such as Fiji, MetaMorph or Cell Profiler to perform image processing tasks. Fiji includes many thresholding methods, for example Otsu's [2]. Recently a method was developed to analyze insulin granules in TEM images [3]. It was developed for a specific (expensive) software package; Definiens. The method described in this paper has a lower miss rate than that of the method used in [3]-17%. A number of approaches for microscopy cell segmentation have been previously described. Methods based on watershed transforms [4], multiscale products [5], and the sliding band filter [6] have been proposed. All these approaches do not address the specific challenges presented.

*shared last author [1]Visual Information Laboratory, [2]Wolfson Bioimaging Facility, [3]School of Biochemistry, [4]School of Physiology and Pharmacology. University of Bristol, Bristol, UK.

We propose a segmentation algorithm which utilizes the level set active contour model, for granule core segmentation of beta islet cell TEM images. Two novel active contour segmentation energy functionals are presented and employed in granule core segmentation. The first proposed level set method includes a novel shape regularizer, to prevent oversegmentation. The second novel contribution is a dual level set active contour based on the energy functional presented in [7]. The core detection algorithm is presented in three steps: a rough segmentation using the first novel contribution, cleaning using morphological operations and an accurate final segmentation using the second novel contribution. Fig. 1 shows a flow chart which outlines the key processes. Once the cores are segmented obtaining their area is trivial. The reminder of the paper is described as follows, Section II describes our level set regularizing term and our dual level set method. Section III presents our algorithm for granule core segmentation. We validate our approach in Section IV and conclude in Section V.

II. THEORETICAL PRELIMINARIES

A. Region Based Fitting Energies

Active contours are a method often used in image segmentation [8]. They were first proposed in [9]. The idea in active contour segmentation models is to evolve a curve subject to constraints from a given image, in order to detect objects in that image.

Chan and Vese proposed a region based energy functional for segmentation, using a level set framework [10]. The Chan-Vese model is unable to correctly segment images with intensity inhomogeneity. A method proposed by Li, et al. is able to deal with inhomogeneity [7]. The method uses a scalable kernel. The kernel K must be nonnegative, $K : \Re^n \rightarrow [0, +\infty)$. Given points u and v the kernel should also have the following properties:

1. $K(-u) = K(u)$;
2. $K(u) \geq K(v)$, if $|u| < |v|$, and $lim_{|u|\rightarrow\infty} K(u) = 0$;
3. $\int K(x)dx = 1$.

In the level set method [11], a contour C is taken as the zero level set of a level set function. Level set values inside the contour are taken as negative and values outside the contour are taken as positive. Given a level set function ϕ and an image I, the local fitting energy for that image is defined as,

$$\varepsilon_{rs}(\phi, f_1, f_2) = \sum_{i=1}^{2} \lambda_i \int \left(\int K(x-y) \left| I(y) - f_i(x) \right|^2 M_i(\phi(y)) dy \right) dx. \quad (1)$$

We define, $M_1(\phi) = H(\phi)$ and $M_2(\phi) = 1 - H(\phi)$, where H is the Heaviside function. λ_1 and λ_2 are two positive constants used to favor segmentations outside and inside the contour respectively, and $f_1(x)$ and $f_2(x)$ are two values that approximate image intensities outside and inside C respectively around x. $I(y)$ are image intensities located in the region around x, which are determined by the size of the kernel. In this experiment a Gaussian kernel is used,

$$K_\sigma(u) = \frac{1}{(2\pi)^{n/2}\sigma^n} e^{-|u|^2/2\sigma^2}, \tag{2}$$

where σ is the standard deviation. The term $K(x-y)$ is a weight term assigned to each point y. Due to the second property of the kernel, the contribution of intensities $I(y)$ to the fitting energy decrease and approach zero as the point y moves farther away from point x. The Gaussian kernel $K_\sigma(x-y)$ is effectively zero when $|x-y| > 3\sigma$. The fitting energy ε_{rs} is a weighted mean square error of the approximation of the image intensities $I(y)$ outside and inside the contour C by the fitting values $f_1(x)$ and $f_2(x)$ respectively, for all points.

B. Internal Energy with Shape Regularization

A localized region based active contour segmentation is applicable to our images because of the inhomogeneity between granules and in some cases within the cytoplasm. There is a lot of fine detail within the cytoplasm which present unwanted information. A new internal energy term is proposed, which is aimed at reducing oversegmentation of insulin granules in TEM images of beta islet cells. The following energy term is proposed:

$$\varepsilon_{in} = \frac{l}{a}, \tag{3}$$

where l is the contours length and a is the contours area. We utilize the fitting energy presented in [7], hence the new energy functional is defined as, $\varepsilon = \varepsilon_{rs} + \varepsilon_{in}$ where ε_{rs} is the energy functional presented in (1). Given a level set function ϕ, the energy ε can be written as:

$$\begin{aligned}\varepsilon(\phi, f_1, f_2) = \quad & \varepsilon_{rs}(\phi, f_1, f_2) + \nu \int |\nabla H(\phi(x))|\, dx \\ & + \mu \int \frac{1}{2}(|\nabla\phi| - 1)^2 dx \\ & + \upsilon \frac{\int |\nabla H(\phi(x))|\, dx}{\int H(\phi(x)) dx}.\end{aligned} \tag{4}$$

Where υ, ν and μ are weighting parameters. $\nu \int |\nabla H(\phi(x))|\, dx$ is a term to keep the contour smooth [10]. The final term is the proposed energy term in (3), presented in a level set framework. In practice, the Heaviside function is approximated by a smooth function H_ϵ defined as:

$$H_\epsilon(x) = \frac{1}{2}[1 + \frac{2}{\pi} arctan(\frac{x}{\epsilon})], \tag{5}$$

and its derivative δ_ϵ as:

$$\delta_\epsilon(x) = \frac{1}{\pi} \frac{\epsilon}{\epsilon^2 + x^2}. \tag{6}$$

where ϵ is a constant. We can define, $M_1^\epsilon(\phi) = H_\epsilon(\phi)$ and $M_2^\epsilon(\phi) = 1 - H_\epsilon(\phi)$. For a given level set function ϕ and

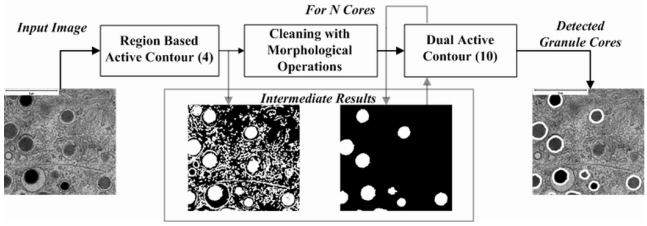

Fig. 1. Granule core detection algorithm using section of TEM image 200×200 pixels.

image I, the energy term $\varepsilon(\phi, f_1, f_2)$ can be minimized with respect to f_1 and f_2 through calculus of variations. The following is obtained:

$$f_i(x) = \frac{K_\sigma(x) * [M_i^\epsilon(\phi(x))I(x)]}{K_\sigma(x) * M_i^\epsilon(\phi(x))}, \quad i = 1, 2. \tag{7}$$

The functions $f_1(x)$ and $f_2(x)$ are weighted averages of values in $I(x)$ whose size is determined by σ.

The regularity of the level set function is important for a stable evolution of the level set function as well as accurate computations [12]. In (4) the third term forces the level set to keep a signed distance function. In [12] the regularization term, $\int \frac{1}{2}(|\nabla\phi| - 1)^2 dx$ was proposed. The term is based on a property of the signed distance function, $|\nabla\phi| = 1$. This will force the level set function to keep signed distance properties as it evolves.

Keeping $f_1(x)$ and $f_2(x)$ fixed ε can be minimized with respect to $\phi(x)$ using the standard gradient decent method, by solving the following gradient flow equation:

$$\begin{aligned}\frac{\partial\phi}{\partial t} \quad = \quad & -\delta_\epsilon(\phi)(\lambda_1 e_1 - \lambda_2 e_2) + \nu\delta_\epsilon(\phi) div(\frac{\nabla\phi}{|\nabla\phi|}) \\ & + \mu(\nabla^2\phi - div(\frac{\nabla\phi}{|\nabla\phi|})) \\ & + \upsilon \frac{a(\delta_\epsilon(\phi) div(\frac{\nabla\phi}{|\nabla\phi|})) + l(\delta_\epsilon(\phi))}{a^2}.\end{aligned} \tag{8}$$

Where e_1 and e_2 are:

$$e_i(x) = \int K_\sigma(y - x) \left|I(x) - f_i(y)\right|^2 dy, \quad i = 1, 2. \tag{9}$$

In the evolution equation the first term is called the data fitting term and is responsible for driving the active contour to the image boundaries. The second term is the length term used for smoothing and the third term is the level set regularization term. The final term is the proposed shape regularizer.

The presented energy functional will reward granule segmentation and penalize cytoplasm segmentation. This is so because it will push the contour to segment structures with larger, area to perimeter ratios. In the case of granule cores in the beta islet TEM images, this is always the case.

C. Dual Region-Scalable Active Contour

During the evolution of a curve, it is quite likely that the curve will pick up undesired objects, and also be trapped in local minima in the image. The dual active contour method uses two active contours, which interact with each other, in order to avoid these short comings. The dual geometric

active contour method presented in [13] utilizes the Chan-Vese active contour. The proposed active contour consists of two contours initialized simultaneously inside and outside the object boundary. In order to deal with inhomogeneous images the energy function in (1) is incorporated into a dual framework. The following energy functional is proposed:

$$\begin{aligned}\varepsilon_{drs}(\phi,\psi) &= \varepsilon_{rs2}(\phi)+\varepsilon_{rs2}(\psi)+ \\ &\quad +\tau\int[H_\epsilon(\phi)-H_\epsilon(\psi)]^2dx. \qquad (10)\end{aligned}$$

Where ϕ and ψ are two level sets, each representing contours initialized inside and outside the object to be segmented respectively. The energy functionals $\varepsilon_{rs2}(\phi)$ and $\varepsilon_{rs2}(\psi)$ are the fitting energies shown in (1) —along with the smoothing term and signed distance regularizer— for level sets ϕ and ψ respectively. τ is a weight for the interaction term. $\varepsilon_{drs}(\phi,\psi)$ is minimized by the gradient decent method with respect to ϕ and ψ, by the solving following the gradient flow equations:

$$\begin{aligned}\frac{\partial\phi}{\partial t} &= -\delta_\epsilon(\phi)(\lambda_1u_1-\lambda_2u_2)+\nu\delta_\epsilon(\phi)div(\frac{\nabla\phi}{|\nabla\phi|}) \\ &\quad +\mu(\nabla^2\phi-div(\frac{\nabla\phi}{|\nabla\phi|})) \\ &\quad -2\tau\delta_\epsilon(\phi)[H_\epsilon(\phi)-H_\epsilon(\psi)], \qquad (11)\end{aligned}$$

$$\begin{aligned}\frac{\partial\psi}{\partial t} &= -\delta_\epsilon(\psi)(\lambda_1v_1-\lambda_2v_2)+\nu\delta_\epsilon(\psi)div(\frac{\nabla\psi}{|\nabla\psi|}) \\ &\quad +\mu(\nabla^2\psi-div(\frac{\nabla\psi}{|\nabla\psi|})) \\ &\quad -2\tau\delta_\epsilon(\psi)[H_\epsilon(\psi)-H_\epsilon(\phi)]. \qquad (12)\end{aligned}$$

Where u_1, u_2 and v_1, v_2 are e_1, e_2 —as stated in (9)— for the level sets ϕ and ψ respectively. The first three terms in each update equation are similar to those defined in Section II-B and the fourth term in each equation is the force which causes the two contours to coincide. Each level set is evolved based on their respective gradient flow equations. The final result is reached when evolution of the level set curves has converged.

III. GRANULE CORE SEGMENTATION

The input for this fully automated algorithm is a beta islet cell TEM image. The proposed region based active contour discussed in Section II-B is applied on the image, as the first step. In order to initialize the active contour a mask is obtained from the image $I(x,y)$. Given the distribution of intensities in I as $D(i), 0\leq i\leq 255$, $D(j)$ the maximum value in $D(i)$ and the cumulative distribution of intensities as $CD(i)$, the mask, Y is calculated as follows:

$$avg = mean(CD(h)), \quad 0\leq h\leq j, \qquad (13)$$

$$CD(b) = avg, \quad Y = I\leq b. \qquad (14)$$

Although applying the active contour in (8) on the TEM beta cell image segments the granule cores, other organelles and grains in the cytoplasm are also segmented. In the second step morphological opening is then applied to the result of the image after active contour segmentation. The opening procedure, along with removing most of the cytoplasm, will also remove other organelles. Objects which are too small are removed as well as objects which are not round enough. The metric used to define roundness is,

$$m = 4\pi\frac{area}{perimeter^2}, \quad m>0. \qquad (15)$$

A perfect circle will have a value of 1 and the less circular the shape the smaller the value. Objects with a roundness less than 0.5 are removed. Some images have granule cores with a lighter center and dark borders. These images are also particularly grainy, even within the granules. In order to remove other organelles in the cytoplasm, as well as fill any granules with a light center, morphological closing is applied, along with image negation. Images which need this extra processing step tend to have a grainy structure. Therefore, in order to decide whether the extra step should be taken, the number of connected components in an image is counted right after applying the active contour in (8) is applied.

In order to capture small dense (dark) granules, that may be missed, $I(x,y)$ is thresholded to highlight values with an intensity less than 55. Connected components in this thresholded image with a roundness less than 0.5 are removed. The result of the previous steps will have a good estimate of the location and shape of the granule cores, however this result may be distorted because of the morphological operations. As a third step in order to accurately segment each granule core the dual region scalable active contour — as described in Section II-C— is applied to each core. Morphological erosion and dilation on each core template are used to obtain initializations for the dual active contour inside and outside the core respectively. To get a complete set of dimensions for an insulin granule, the granule halo area needs to be measured. We present a novel method for granule halo segmentation of beta islet cell TEM images in [14].

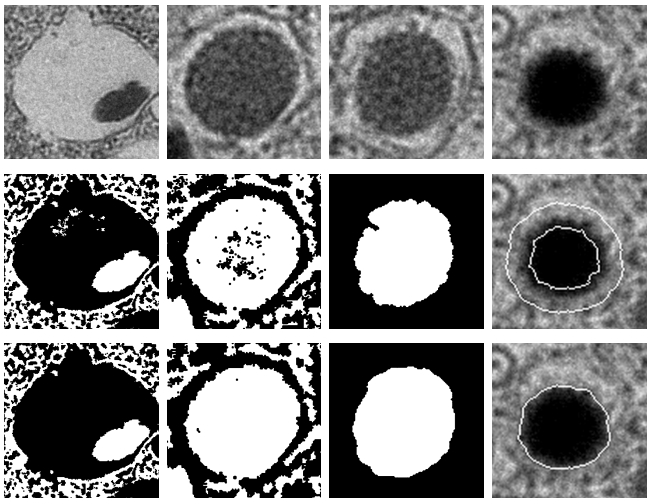

Fig. 2. Columns 1 and 2 compare the region scalable active contour without shape regularizer [7], and with shape regularizer (8), middle row and last row respectively. Column 3 demonstrates the use of the dual active contour in Section II-C. The middle row shows a distorted core after the cleaning step. This distortion is corrected by the dual active contour as seen in the third row. Column 4 shows a granule core, dual contour initializations and the final segmentation, from top to bottom respectively.

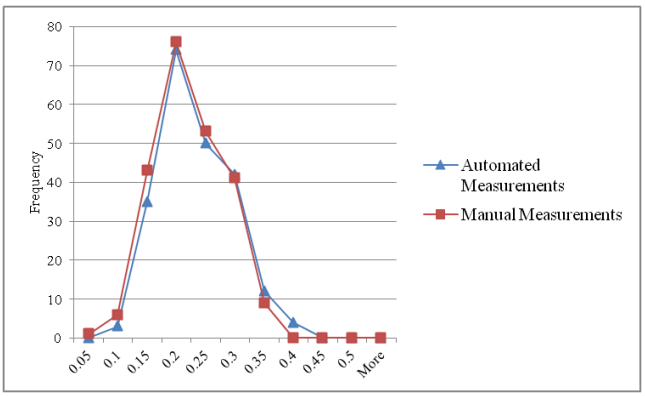

Fig. 3. Granule core radii distributions for a TEM image of a chemically fixed beta islet cell. The horizontal axis is the radii bins in μm, while the vertical axis is frequency.

IV. Results

Our algorithm is initially applied to five images, two fixed chemically and three fixed using high pressure fixation. Each image is 5000×5000 pixels. This number of images gives about 1300 granules to be processed. Fig. 2 demonstrates the effectiveness of our novel active contour models. In step 1 for all images $\nu = 0.003 \times 255 \times 255$, $\mu = 1$, $\lambda_1 = 1$, $\lambda_2 = 1$, $\sigma = 7$, $\epsilon = 1$, $\triangle t = 0.1$ and $\upsilon = 15.38 \times 255 \times 255$. A small scale size is chosen because greater detail is picked up. For the dual active contour, μ, λ_1, λ_2, σ, ϵ and $\triangle t$ are the same as step 1, while $\nu = 0.005 \times 255 \times 255$ and $\tau = 2.5 \times 255 \times 255$. For all morphological operations a disk shaped structuring element is used.

As a final step the same images are also manually analyzed and the results compared with the automated analysis. A core detection rate of 97.12% was observed. Of the total number of cores detected automatically, 12.3% were misses and 9.9% were false positives. The number of insulin granules in beta islet cells is already known to be about 6000 [3]. Ultimately statistics on granule sizes are needed for analysis. In order to check the effectiveness of our algorithm we compared the average granule core areas, with those done manually. The metric used to record granule sizes is a radius of a circle with the same area as the granule core. Fig. 3 shows the distributions of granule core areas, from a single TEM beta islet cell image. The average granule core radii error is 8.22% for all images. Table. I summarizes our results on radii distributions for cores, on all five images.

V. Conclusion

In this paper we present an automatic segmentation approach for insulin granule cores in TEM images of beta islet cells. In our core segmentation algorithm we present two novel active contour models. The first is a localized region based energy with a shape regularizer to help reduce oversegmentation in the TEM images. The second contribution is a localized region based dual active contour, which is able overcome inaccurate segmentations due to image inhomogeneity. Core segmentation is separated into three steps: pre-segmentation, morphological cleaning and an accurate final segmentation. The method gives a detection rate of 97.12%. In order to check the accuracy of our segmentations, the resulting granule areas are compared to a manually obtained ground truth. An average area difference of 8.22% between the automated results and the ground truth is observed. Having an automated approach for microscopy segmentation can help biologists get quantitative information faster, it also removes human error from the process as well as makes it completely reproducible.

TABLE I

M = Mean, SD = Standard Deviation, CF = Chemically fixed, HPF = High pressure fixation.

	Proposed Algorithm		Ground Truth	
	M (μm)	SD(μm)	M (μm)	SD(μm)
CF 1	0.20884	0.05860	0.19843	0.05847
HPF 1	0.23768	0.04872	0.24254	0.04965
CF 2	0.17431	0.03892	0.15214	0.04085
HPF 2	0.15166	0.04705	0.18203	0.05166
HPF 3	0.20254	0.04759	0.21258	0.06141

References

[1] X. Zhou and S.T.C. Wong, "Informatics challenges of high-throughput microscopy," *Signal Processing Magazine, IEEE*, vol. 23, no. 3, pp. 63 –72, May 2006.

[2] N. Otsu, "A threshold selection method from gray-level histograms," *Systems, Man and Cybernetics, IEEE Transactions on*, vol. 9, no. 1, pp. 62 –66, Jan. 1979.

[3] E. Fava, J. Dehghany, J. Ouwendijk, A. Müller, A. Niederlein, P. Verkade, M. Meyer-Hermann, and M. Solimena, "Novel standards in the measurement of rat insulin granules combining electron microscopy, high-content image analysis and in silico modelling," *Diabetologia*, vol. 55, pp. 1013–1023, 2012, 10.1007/s00125-011-2438-4.

[4] H. Nguyen and Q. Ji, "Shape-driven three-dimensional watersnake segmentation of biological membranes in electron tomography," *Medical Imaging, IEEE Transactions on*, vol. 27, no. 5, pp. 616 –628, May 2008.

[5] J.-C. Olivo-Marin, "Extraction of spots in biological images using multiscale products," *Pattern Recognition*, vol. 35, no. 9, pp. 1989 – 1996, 2002.

[6] P. Quelhas, M. Marcuzzo, A.M. Mendonca, and A. Campilho, "Cell nuclei and cytoplasm joint segmentation using the sliding band filter," *Medical Imaging, IEEE Transactions on*, vol. 29, no. 8, pp. 1463 – 1473, Aug. 2010.

[7] C. Li, C.Y. Kao, J.C. Gore, and Z. Ding, "Minimization of region-scalable fitting energy for image segmentation," *Image Processing, IEEE Transactions on*, vol. 17, no. 10, pp. 1940 –1949, Oct. 2008.

[8] N. Volkmann, "Chapter two - methods for segmentation and interpretation of electron tomographic reconstructions," *Cryo-EM, Part C: Analyses, Interpretation, and Case studies*, vol. 483, pp. 31 – 46, 2010.

[9] M. Kass, A. Witkin, and D. Terzopoulos, "Snakes: Active contour models," *International Journal of Computer Vision*, vol. 1, no. 4, pp. 321–331, 1988.

[10] T.F. Chan and L.A. Vese, "Active contours without edges," *Image Processing, IEEE Transactions on*, vol. 10, no. 2, pp. 266 –277, Feb 2001.

[11] S. Osher and J.A. Sethian, "Fronts propagating with curvature dependent speed: Algorithms based on hamilton-jacobi formulations," *Journal of Computational Physics*, vol. 79, no. 1, pp. 12–49, 1988.

[12] C. Li, C. Xu, C. Gui, and M.D. Fox, "Level set evolution without re-initialization: a new variational formulation," *Computer Vision and Pattern Recognition, 2005. CVPR 2005. IEEE Computer Society Conference on*, vol. 1, pp. 430 – 436 vol. 1, June 2005.

[13] G. Zhu, Q. Zeng, and C. Wang, "Dual geometric active contour for image segmentation," *Optical Engineering*, vol. 45, no. 8, pp. 080505, 2006.

[14] D. Nam, J. Mantell, D. Bull, P. Verkade, and A. Achim, "Segmentation and analysis of insulin granule membranes in beta islet cell micrographs," in *Proc. EUSIPCO, Bucharest, Romania*, August 2012.